Bifurcation Analysis of a Driven *R-L-Diode* Circuit

田中　聡、野口　淳、樋口　信一、松本　隆

Satoshi TANAKA, Jun NOGUCHI, Shin-ichi HIGUCHI and Takashi MATSUMOTO

Department of Electrical Engineering, Waseda University, Tokyo, 169, Japan

SUMMARY

The paper reports *multi-folding*, a new chaotic attractor formation mechanism in a driven *R-L-Diode* circuit. This mechanism is responsible for the alternative appearance of period-one attractors and chaotic attractors in the bifurcation diagram. After several simplification of the dynamics, exact bifurcation equations are derived and analyzed. It turns out that all the period-one attractors of our interest belong to the same family. Extensive measurements are performed to simplify the dynamics to a one-dimentional mapping without loosing essential features of the observed bifurcation diagrams. The period-one attractor of this map also belong to the same family. The *multi-folding*, when couched in terms of the simplified one-dimensional map is characterized by its *multi-modality*.

I. INTRODUCTION

The purpose of this paper is to report a new mechanism, called multi-folding, for chaotic attractor formation in a driven *R-L-Diode* circuit. In spite of its simplicity, the driven *R-L-Diode* circuit given in Fig. 1 exhibits a very rich variety of interesting phenomena [1-17], including period doubling, chaotic attractor, intermittency and crisis. One of the most interesting features of the bifurcation diagram associated with this is that the large periodic windows and the chaotic bands alternate while the period increases exactly by one (Fig.2). It has been demonstrated that a "folding" mechanism is responsible for this phenomenon [16]. Several other works [6,9,17] have pointed out that qualitatively different bifurcations are taking place at the lower frequency region of the bifurcation diagram. Figure 3 is the one-parameter bifurcation diagram of the circuit which motivated the present study. The horizontal axis is the amplitude of

1

sinusoidal voltage source while the vertical axis is the current of the circuit sampled at a particular phase of the sinusoidal voltage source. The circuit parameters are;

$R=75\ \Omega$, $L=2.5$ mH, Diode: 3CC13,

DC bias voltage $E_b=-1.0$ V $f = 25$ kHz, $0 \le E \le 4.0$ V.

This bifurcation diagram is qualitatively different from Fig. 2, in that rather than increasing the period of each successive periodic windows by one, period-1 windows (e.g., (a), (b) and (c)) and chaotic bands appear alternatively. Namely, something qualitatively different is happening at lower frequencies.

Our approach in the present work is (1) to apply exact bifurcation equation to the simplified dynamics and analyze period-one orbits (not only attractors but also repellers), (2) and to carefully observe the chaotic attractors and construct a simple one-dimensional *discrete map* model which captures the important qualitative features of the observed bifurcation phenomena. The mechanism of our interest, in terms of the one-dimensional map model, turns out to be its multi-modality. This, in turn, translates back to a "multi-folding" mechanism in the original dynamics.

II. THE DYNAMICS

A fairly accurate equivalent circuit of a junction diode is given by a parallel connection of three nonlinear elements [18]:

(1) nonlinear resistor

$$I_d = I_s\ (\exp(q'v/kT)\text{-}1) \tag{1}$$

(2) junction capacitor $C_j(v)$ due to the depletion region;

$$C_j(v) = C_{j0}/(1\text{-}v/V_{j0})^{1/2} \tag{2}$$

(3) diffusion capacitor C_d (v) due to the rearrangement of the minority carrier density

$$C_d(v) = C_{d0}\exp(q'v/kT) \tag{3}$$

where I_s, q', k, T, V_{j0}, C_{j0} and C_{d0} are the saturation current, electron charge, Boltzmann constant, the absolute temperature, the potential voltage of the pn junction, the junction capacitance at zero bias and the diffusion capacitance at zero bias, respectively.

Note that under reverse bias, the capacitor is dominated by the *junction* capacitor (2), whereas under forward bias, the capacitor is dominated by the *diffusion* capacitor (3). By measurements the capacitance is found to be 51.4 nF at 0.5 V (a positive bias) and 235 pF at -1.0 V (a negative bias). Note that the difference in the capacitance

values is more than two orders of magnitude. The diode exhibits also a rectification characteristic (1) : in the reverse bias region the resistance is almost infinite, whereas in the forward bias region the resistance is very small. For example at 0.5 V the resistance is 100 Ω. By carefully measuring the impedances of the capacitors and the resistor over a frequency range of more than 25 kHz, it was found that the impedances of the capacitors are much smaller than that of the resistor. Therefore the diode characteristic can be simplified and modeled by a 2-segment piecewise-linear capacitor [10] so that the dynamics of the R-L-Diode circuit can be accurately described by

$$\frac{dq}{dt} = i$$

(4)

$$L\frac{di}{dt} = -Ri - \left\{ \begin{array}{ll} \frac{1}{C_d}q & \text{if } q \geq 0 \\ \frac{1}{C_j}q & \text{if } q < 0 \end{array} \right\} - E_d + E_b + E\sin(2\pi ft)$$

where C_d is the diffusion capacitance at 0.5 V bias, C_j is the junction capacitance at -1.0 V, $E_d = 0.5$ V is the break point voltage at which the capacitance value changes between the junction capacitance and the diffusion capacitance, i is the circuit current and q is the charge of the capacitor.

III. EXACT BIFURCATION EQUATIONS

To observe period-one attractor more clearly , we will derive *exact* bifurcation equations of the simplified dynamics (4) of our R-L-Diode circuit, based on the piecewise-linear normal form theorem[19-20].

In order to apply the normal form theorem, we first, rescale the dynamics(4) and convert it into the *fourth-order autonomous* system as follows;

$$\frac{dQ}{d\tau} = I$$

$$\frac{dI}{dt} = -kI - \left\{ \begin{array}{ll} \frac{1}{C_j}Q & \text{if } Q < 1 \\ \frac{1}{C_d}Q - \frac{1}{C_d} + \frac{1}{C_j} & \text{if } Q \geq 1 \end{array} \right\} + \frac{E}{C_j(E_b-E_d)}M$$

$$\frac{dM}{d\tau} = N$$

(5)

$$\frac{dN}{d\tau} = -M$$

where

$$Q \equiv \frac{\omega^2 L}{C_j \; E_b\text{-}E_d} q + 1 \; , I \equiv \frac{\omega L}{C_j \; E_b\text{-}E_d} i \; , \tau \equiv \omega t , k \equiv \frac{R}{\omega L} , \frac{1}{C_x} \equiv \frac{1}{\omega^2 C_x L} \; (x = d, j)$$

$$M \equiv \sin \tau , N \equiv \cos \tau , M^2 + N^2 = 1.$$

Next, we recast (5) as follows;

$$\frac{dx}{d\tau} = \begin{cases} Ax & (Q \geq 1) \\ Bx & +p & (Q < 1) \end{cases} \tag{6}$$

where

$$x = (Q, I, M, N)^{\mathrm{T}} , \; p = (0, \frac{1}{C_d} \frac{1}{C_j} , 0, 0)^{\mathrm{T}} ,$$

(T indicates transpose of a vector.)

$$A = \begin{bmatrix} 0 & 1 & 0 & 0 \\ -\frac{1}{C_j} & -k & \frac{E}{C_j \; (E_b\text{-}E_d)} & 0 \\ 0 & 0 & 0 & 1 \\ 0 & 0 & -1 & 0 \end{bmatrix} \qquad B = \begin{bmatrix} 0 & 1 & 0 & 0 \\ -\frac{1}{C_d} & -k & \frac{E}{C_j \; (E_b\text{-}E_d)} & 0 \\ 0 & 0 & 0 & 1 \\ 0 & 0 & -1 & 0 \end{bmatrix}$$

Figure 4 shows a schematic picture of an orbit in the (Q, I) space. Consider a point X lying on the boundary B_0. Let Y and Z be the points where the trajectory starting from X hits B_0 again at positive time s_1 and negative time $-t_1$, respectively. Similarly let W be the point where the trajectory starting from Y hits B_0 again at positive time u_1. Since the system is linear in each region, we have

$$Y = e^{Ds_1} X$$
$$Z = e^{-At_1} X$$
$$W = e^{Au_1} Y = e^{Au_1} e^{Ds_1} X$$

where

$$D=A^{-1}BA$$

Since **X** , **Y** and **W** all lie on the boundary B_0,

$$<\alpha, X>=1 \ , \ <\alpha, e^{Ds1}X>=1 \ , \ <\alpha, e^{-At1} X>=1, \quad <\alpha, e^{Au1}e^{Ds1} X>=1$$

where $<,>$ denotes inner product and $\alpha =(1,0,0,0)^T$. Therefore

$$X=(e_1\alpha^T+ e_2\alpha^T e^{Cs1}+ e_3\alpha^T e^{-At1}+ e_4\alpha^T e^{Au1}e^{Ds1})^{-1}(1,1,1,1)=k(s_1,t_1,u_1)h \quad (7)$$

where

$$e_1=(1,0,0,0)^T , \ e_2=(0,1,0,0)^T , \ e_3=(0,0,1,0)^T , \ e_4=(0,0,0,1)^T .$$

Now, if the trajectory starting from **Z** hits the point **V** on the boundary B_0 at a negative time $-s_2$, then **V** is given by

$$V= e^{-Ds2}Y=e^{-Ds2}e^{-At1}X.$$

If this orbit is periodic, then **W**=**V** which is equivalent to

$$(e^{Au1}e^{Ds1} - e^{-Ds2}e^{-At1})X=0.$$

Consequently, a periodic orbit is characterized by

$$(e^{Au1}e^{Ds1} - e^{-Ds2}e^{-At1}) k(s_1,t_1,u_1)h =0 \qquad (8)$$

$$\{e_3 k(s_1,t_1,u_1)h \ \}^2+\{e_4 k(s_1,t_1,u_1)h \ \}^2=1 \qquad (9)$$

Note that there are only three (out of four) independent equations in (8) because the third and fourth components of **W** and **V** are dependent through (9).

It is shown rigorously in Ref.[20] that eigenvalues of the Poincare return map on B_0 is given by the eigenvalues of $\Phi=e^{At1}e^{Cs2}e^{Au1}e^{Cs1}$. One of the four eigenvalues is always 1 because (M , N) is always periodic (see (7)). If **X** is a periodic point, one of the remaining three eigenvalues is also 1. Note that a saddle node bifurcation(resp.

period doubling bifurcation) is characterized by the fact that one of the remaining two eigenvalues is 1(resp. -1). Therefore

$3 - Tr + Det = 0$ (resp. $-1 - Tr + Det = 0$)

$$(e^{Au_1}e^{Cs_1} - e^{-Cs_2}e^{-At_1}) k(s_1,t_1,u_1)h = 0 \qquad (10)$$

$$\{e_3 k(s_1,t_1,u_1)h\}^2 + \{e_4 k(s_1,t_1,u_1)h\}^2 = 1$$

where

$Tr = trace(\Phi)$, $Det = determinant(\Phi)$.

As will be pointed out in Section IV, the ratio between the time a trajectory spends in the C_j-region and the time the trajectory spends in the C_j-region plays an important role in characterizing a trajectory. In order to take this into account let S be the time a trajectory spends in the C_d-region (i.e. $Q \geq 1$), and let T be the time a trajectory spends in the C_j-region ($Q < 1$), and let us look at the ratio S/T ($S + T = 2\pi$) as E is varied.

Figure 5 shows one-parameter bifurcation diagram of a period-one attractor which is calculated by solving the exact equations. The circuit parameters are

$R = 214\ \Omega$, $L = 2.5$ mH, $C_j = 235$ pF, $C_d = 51.4$ nF, $\quad f = 30$ kHz $E_b = -1.0$ V.

The horizontal axis is the voltage source amplitude E, the vertical axis is S/T. The bifurcation structures of our interest are clearly captured. In Fig.5, a solid(resp.broken) line indicates that the period-one attractor is stable(resp. unstable). As E increases, the following sequence is repeated: period-one saddle-node bifurcation

$\rightarrow$ stable period-one orbit $\rightarrow$ unstable period-one orbit $\rightarrow$ stable period-one orbit $\rightarrow$ period-one saddle-node bifurcation. It is clear that the period-one attractors are all conected in the ($E,S/T$)-space and belong to the same family.

III. OBSERVATION OF THE ATTRACTOR

In order to uncover the attractor formation mechanism, various cross sections of the attractor are measured. Shown in Fig.6 are the cross sections measured at different phases of the input sinusoidal waveform where $E = 2.4$ V, $f = 50$ kHz. The horizontal axis is the diode voltage v_d and the vertical axis is the current i. The phases are increased in the order of (a), (b),---(f).

In order to clarify the effects of circuit parameters on the dynamics, let us perform the following rescaling on (4);

$$Q \leftarrow (Lf^2/E)q, \quad I \leftarrow (Lf/E)i, \quad \tau \leftarrow ft. \tag{11}$$

The dynamics (4) is rewritten as

$$\frac{dQ}{d\tau} = I$$

$$\frac{dI}{d\tau} = \frac{R}{fL}I - \left\{ \begin{array}{ll} \frac{1}{f^2 L C_d}Q & \text{if } Q \geq 0 \\ \frac{1}{f^2 L C_j}Q & \text{if } Q < 0 \end{array} \right\} - \frac{(E_d - E_b)}{E} + sin(2\pi\tau) \tag{12}$$

The fact that $C_j = 235$ pF $\ll C_d = 51.4$ nF gives rise to two important features to (12).

(i) The vertical component of the vector field (Q, I) on $Q < 0$ is much faster than that on $Q \geq 0$.

(ii) Since the imaginary part of the eigenvalues on $Q < 0$ (resp. $Q \geq 0$),

$$\frac{\sqrt{\frac{4L}{C_j} - R^2}}{2fL} \quad \left(\text{resp.} \quad \frac{\sqrt{\frac{4L}{C_d} - R^2}}{2fL} \right)$$

the resonant frequency on $Q < 0$ is much higher than that on $Q \geq 0$. This means that, there is a strong "twisting" mechanism on $Q < 0$.

From (11) and (12) v_d is given as

$$v_d = \left\{ \begin{array}{ll} \frac{E}{f^2 L C_d}Q & \text{if } Q \geq 0 \\ \frac{E}{f^2 L C_j}Q & \text{if } Q < 0 \end{array} \right\} + E_d \tag{13}$$

where $C_j = 235$ pF $\ll C_d = 51.4$ nF. Therefore the part on $v_d \geq E_d$ is compressed in the horizontal direction strongly. To help understanding the transformation process, Fig. 7 gives the geometric structure corresponding to each figure in Fig.6, where the small triangle shows the reference orientation, and the vertical line indicates $Q = 0$ ($v_d = E_d$), i.e., the boundary between the diffusion capacitance region (right) and the junction capacitance region (left).

(a) The attractor is in the region which is dominated by the diffusion capacitor.

(b) A part of the attractor moves into the region which is dominated by the junction capacitor. It follows from (i) and (ii) above that when the attractor moves from the diffusion capacitor region into the junction capacitor region, it is stretched because of

the difference of the vector fields. And then it is twisted in the clockwise direction.

(c) The attractor is further twisted.

(d) The attractor is stretched again and twisted.

(e) The attractor is further twisted (see Fig.8 (a) for a blown up picture).

(f) The attractor is squeezed and finally the attractor returns to the initial region (see Fig.8 (b) and (c) for two intermediate blown up pictures between (e) and (f)).

Thus (a) - (f) is summarized as : stretching and twisting give rise to a folded object. It is clear that the attractor is folded twice.

It is, therefore, easy to infer that the attractor could be twisted many times. This can happen, for instance, when E becomes smaller. This is due to the fact that the bias term in (12) shifts the dynamics to the left and hence gives rise to a larger time period on which the attractor spends in the $Q < 0$ $(v_d < E_d)$ region. Therefore the attractor could be twisted more times ("multi-folding" (Fig. 9 (a))).

IV. ONE-DIMENSIONAL MAP

Now our question is how the "multi-folding" generates the alternative appearance of period-1 attractors and chaotic attractors in the bifurcation diagram. To answer the question, we now propose the one-dimensional map (Fig. 9 (b)) :

$$x_{n+1} = a(1 - \cos b(1 - x_n)) \qquad (14)$$

as a model capable of reproducing the dynamics in Fig.9 (a).

In order to show that (14) captures all the important features of the observed bifurcations, we will discuss the dependencies of a and b on E and f only roughly for our present purpose. Our analysis is based upon laboratory measurements.

(i) *parameter a*

This parameter controls the extrema of the mapping. In other words a controls the size of the attractor. From the observations of Fig.3 the size of the attractor is proportional to E. Therefore a should be proportional to E, the amplitude of the voltage source. Moreover, a is inversely proportional to the circuit dissipation which is given by $\exp(R/2fL)$ [16]. Therefore

$$a \propto (E + a_1) \exp(-R/2fL) \qquad (15)$$

would be an appropriate relationship, where a_1 is a parameter.

(ii) *parameter b*

This parameter controls the number of extrema of (14) which corresponds to the

number of twisting in the junction capacitor region. The latter should be proportional to the imaginary part ω_j of the eigenvalue of the junction capacitor region, and the length t_j of the time interval on which the attractor stays in the junction capacitor region; namely,

$$b \propto \omega_j \cdot t_j + \theta \tag{16}$$

where θ represents the phase constant. When E is decreased, as mentioned before, the bias term in (12) shifts the dynamics to the left and hence gives rise to a larger time period t_j. Therefore t_j is inversely proportional to the amplitude E. When E is increased it has been observed that the change of the number of twisting becomes more moderate. This factor is represented by θ, and the relationship

$$\theta \propto b_1(1 - b_2/(E + b_2)) \tag{17}$$

seems reasonable, where b_1 and b_2 are parameters. Therefore we will write (10) as

$$b \propto \frac{\sqrt{\frac{4L}{C_j} - R^2}}{2fL} \frac{b_3}{E + b_3} + b_1(1 - \frac{b_2}{E + b_2}) \tag{18}$$

where b_3 is another parameter.

Figure 10 shows the bifurcation diagrams of (14) where the horizontal axis is E and the vertical axis is x_n. The parameter values are chosen as follow :

$$R = 214 \ \Omega \ ; \ C_2 = 235 \ \text{pF}; \ L = 2.50 \ \text{mH}; \ a_1 = 0.15; b_1 = 2.4; \ b_2 = 1.0 \ ; b_3 = 0.2$$

The frequency of the voltage source is fixed at $f=35$ kHz, while the amplitude of the voltage source is varied from 1.5 V to 0.0 V. Observe that the basic qualitative features of Fig.3 are clearly captured. In particular, period-one windows and chaotic bands appear alternatively. Figure 11 (a)-(c) show the orbits of (14) at the parameter values indicated as (a)-(c), respectively in Fig.3 and Fig. 10. It is clear that (14) undergoes a saddle-node bifurcation when it becomes tangent to the diagonal line. Since the extremum value of (14) is determined by the parameter a and since a is monotonic with respect to E (see (15)), the only possible reason for (14) to undergo repeated period one saddle-node bifurcations is its multi-modality. Namely, the hills and valleys of (14) become tangent to the diagonal one by one. Therefore it is clear that these period-one attractors belong to the same family. The qualitative features of Fig.5 are also clearly captured. In terms of the original circuit dynamics, this means that an

120

initial rectangle is mapped into a "multi-folded object" (see Fig.8,9), *i.e.* multi-folding.

Finally we would like to thank Motomasa Komuro of Nishi-Tokyo University for many constructive discussions.

REFERENCES

[1] P.S.Linsay, **Phys. Rev. Lett.** 47 (1981) 1349.

[2] J.Testa, J.Perez and C.Jeffries, **Phys. Rev. Lett.** 48 (1982) 714.

[3] R.W.Rollins and E.R.Hunt, **Phys. Rev. Lett.** 49 (1982) 1295.

[4] S.D.Bronson, D.Dewey and P.S.Linsay, **Phys. Rev. A** 28 (1983) 1201.

[5] H.Ikezi, J.S.deGrassie and T.H.Jenson, **Phys. Rev. A** 28 (1983) 1207.

[6] J.Cascais, R.Dilao and A.Noronha Da Costa, **Phys. Lett. A** 93 (1983) 213.

[7] E.R.Hunt and R.W.Rollins, **Phys. Rev.** A29 (1984) 1000.

[8] T.Klinker, W.M.Ilse and W.Lauterborn, **Phys. Lett. A** 101 (1984) 371.

[9] M.F.Bocko, D.H.Douglass and H.Frutchy, **Phys. Lett. A** 104 (1984) 388.

[10] T.Matsumoto, L.O.Chua and S.Tanaka, **Phys. Rev. A** 30 (1984) 1155.

[11] T.H.Yoon, J.W.Song, S.Y.Shin and J.W.Ra, **Phys. Rev. A** 30 (1984) 3347.

[12] C.D.Jeffries, **Phys. Scri.** T9 (1985) 11.

[13] S.Tanaka, T.Matsumoto and L.O.Chua, **Proc. IEEE Int. Symp. on Circuit and Systems** (1985) 851.

[14] J.M.Perez, **Phys. Rev. A** 32 (1985) 2990.

[15] J.Mevissen, R.Seal and L.Waters, **Phys. Rev. A** 32 (1985) 2990.

[16] S.Tanaka, T.Matsumoto and L.O.Chua, **Physica D** 28 (1987) 317.

[17] J.H.Baxter, M.F.Bocko and D.H.Douglass, **Phys.Rev. A** 41 (1990) 619.

[18] E.S.Yang, Fundamentals of Semiconductor Devices (McGraw-Hill, New York, 1987).

[19] M.Komuro, **Japan J. Appl. Math.**, vol.5, no.2, pp.257-304 (1988).

[20] M.Komuro, **Japan J. Appl. Math.**, vol.5, no.3, pp. 503-549 (1988) .
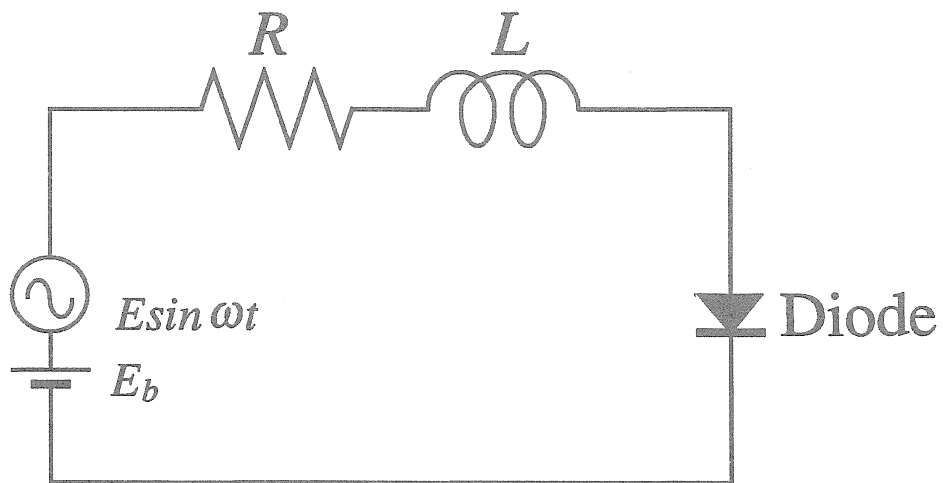
Figure 1 A driven *R-L-Diode* Circuit.

Figure 2 One-parameter bifurcation diagram.

The source frequency f = 140 kHz and the dc bias E_b = 0 V. The horizontal axis is the amplitude of the voltage source E (0.5 V/div) and the vertical axis is the inductor current i_L (2.0 mA/div).
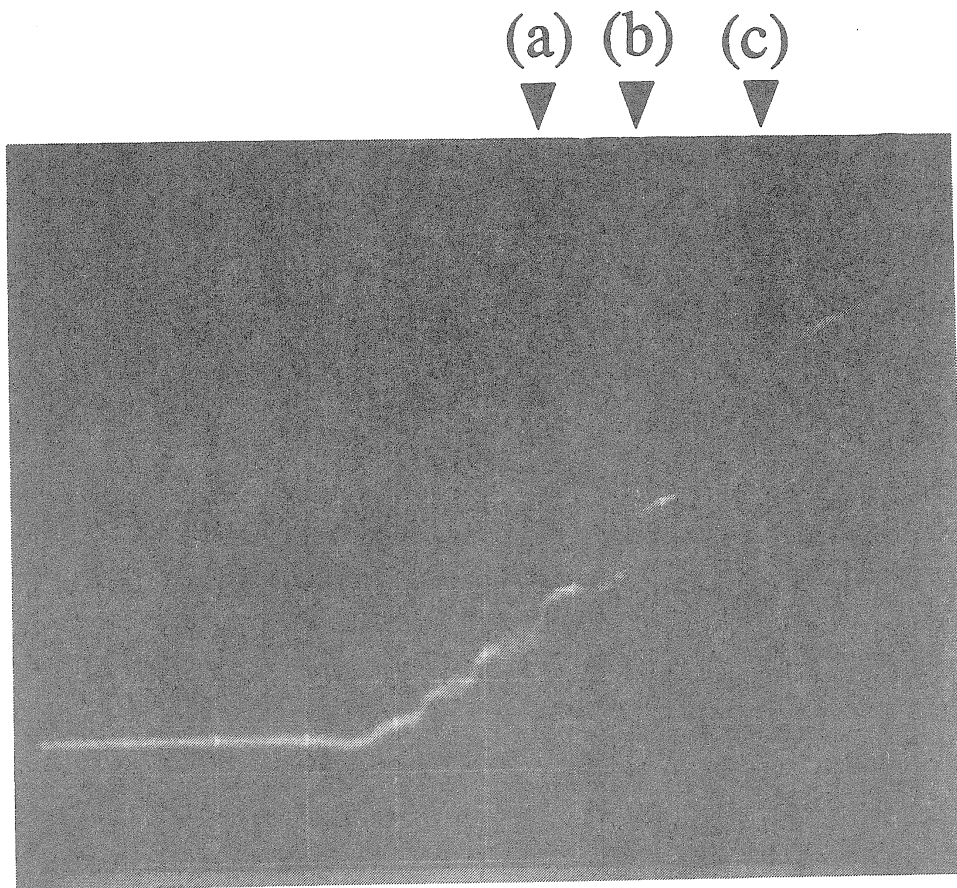
Figure 3 One-parameter bifurcation diagram.
The source frequency f = 25 kHz and the dc bias Eb = -1.0 V. The horizontal axis is the amplitude of the voltage source E (0.5 V/div) and the vertical axis is the inductor current i_L (2.0 mA/div).
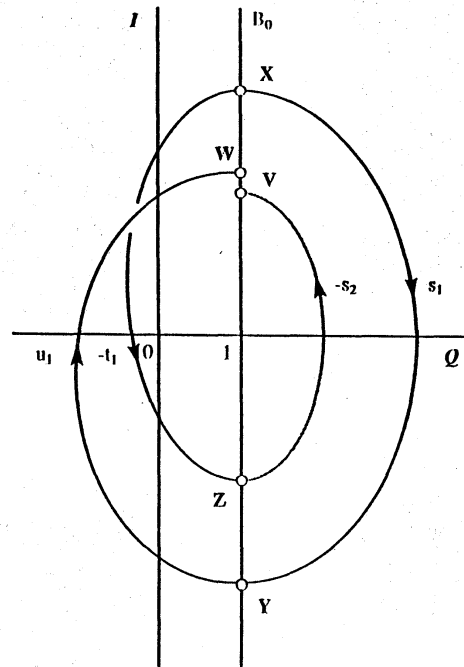
Figure 4 Schematic picture of orbit in (Q,I)-space. The horizontal axis is I, and the vertical axis is Q. B_0 indicates boundary line, $Q = 1$.
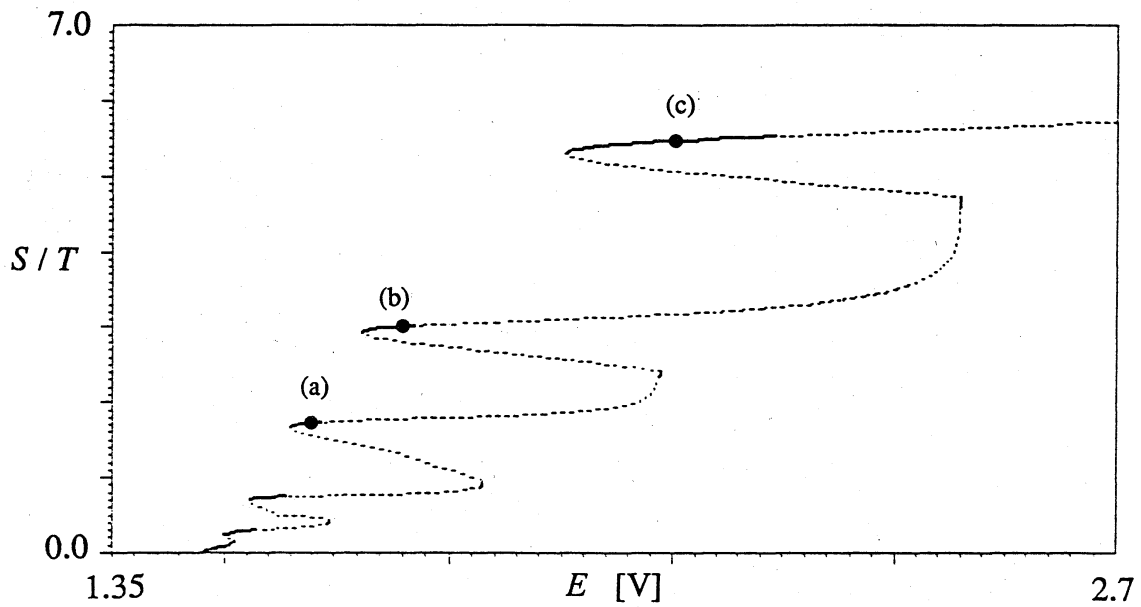
Figure 5 One-parameter bifurcation diagram at $f = 30$ kHz.
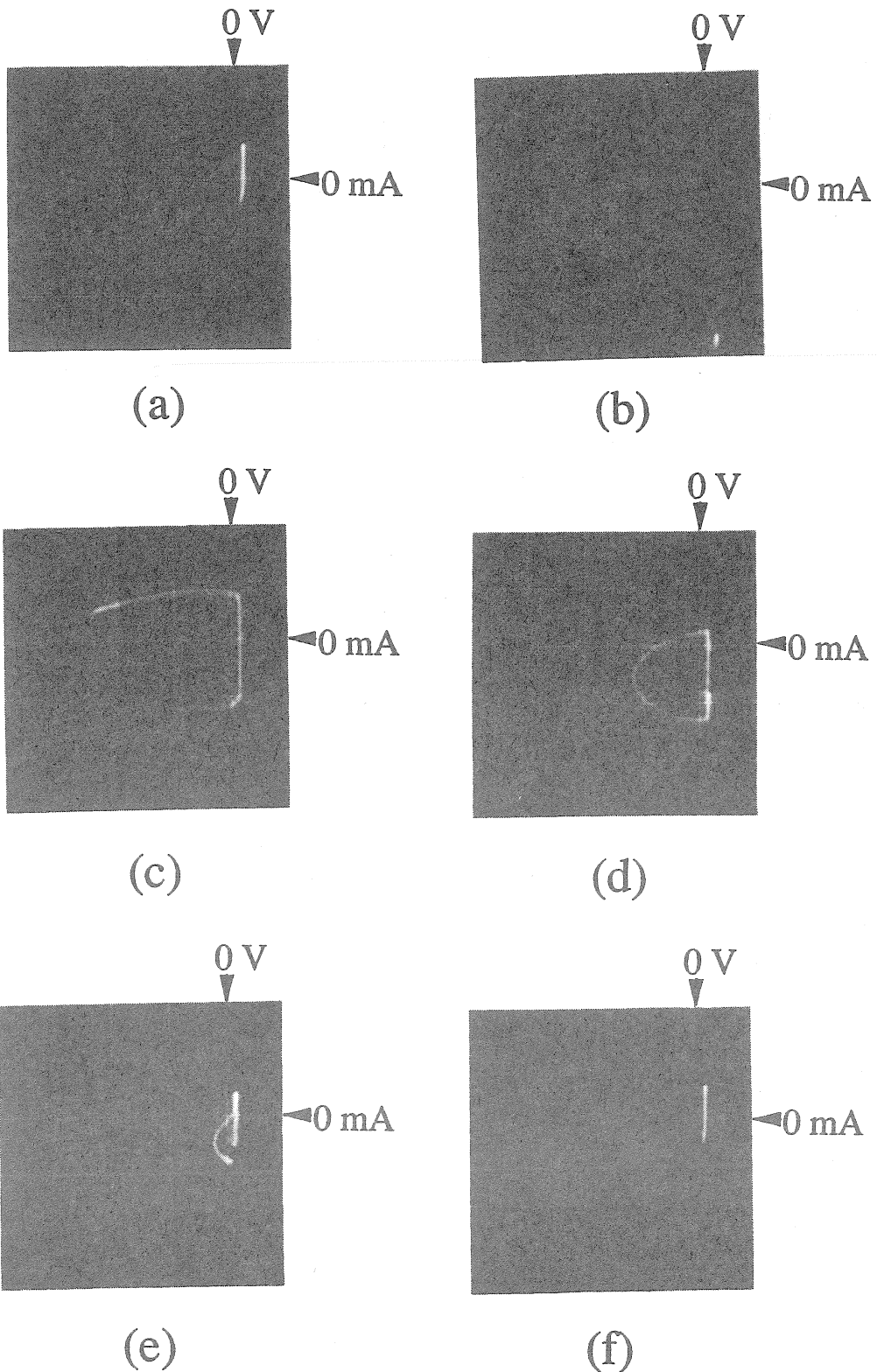
Figure 6 Observed cross sections of the *R-L-Diode* circuit at *E*=2.4 V, *f*=50 kHz. The horizontal axis is the diode voltage v_d (5.0 V/div) and the vertical axis is the inductor current i_L (2.0 mA/div). Since the origin is not located at the center of each figure, the axes are indicated by arrows.
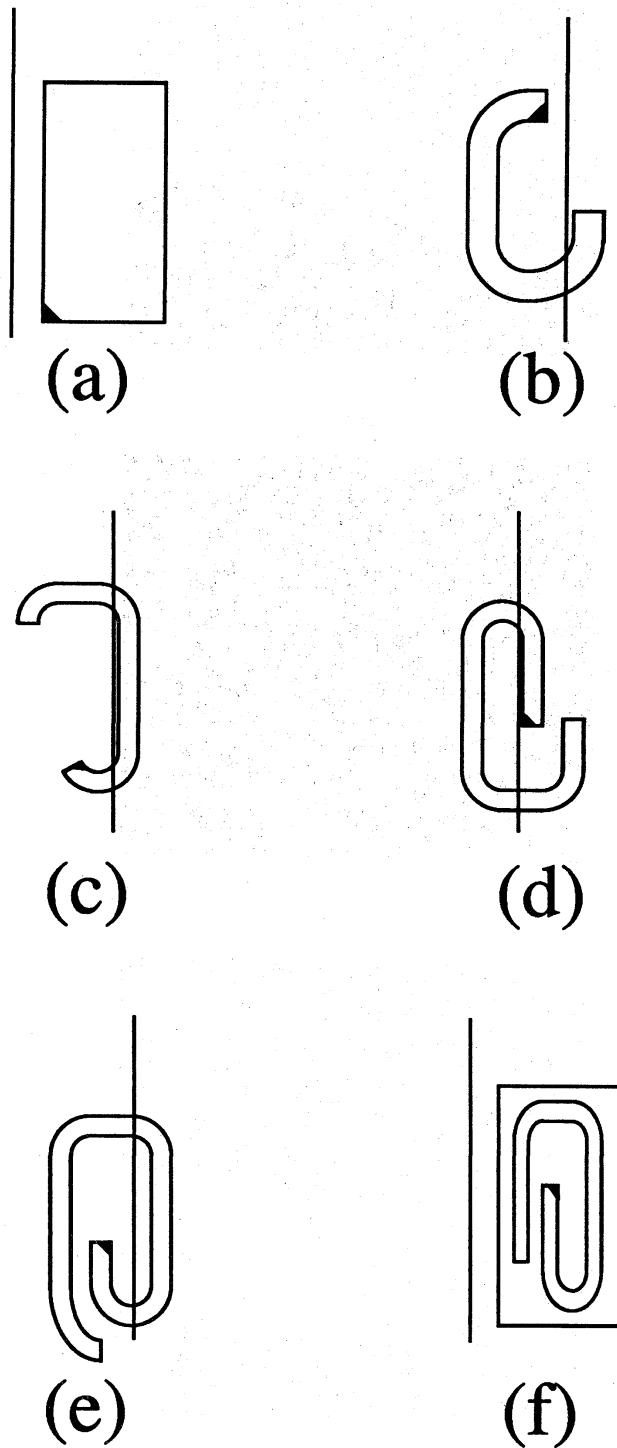
Figure 7 Geometric model of the attractor formation. Each figure corresponds to the one in Fig.6.

0 V

◄0 mA
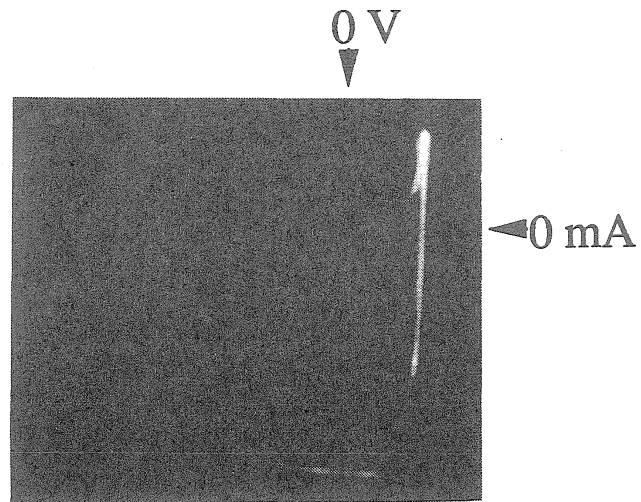
(a)
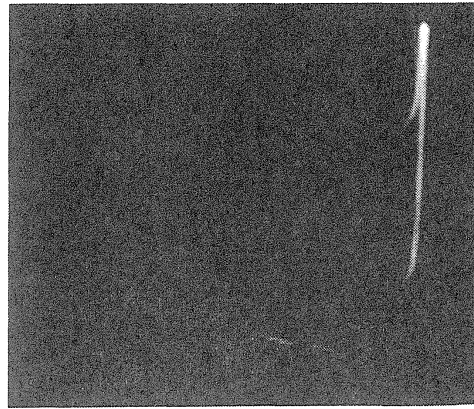
(b)
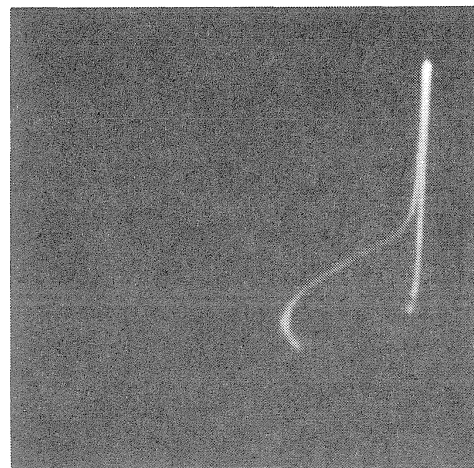
(c)

Figure 8 Blown up cross sections at E=2.4 V, f=50 kHz.

The horizontal axis is the diode voltage v_d (0.5 V/div) and the vertical axis is the inductor current i_L (0.5 mA/div). Since the origin is not located at the center of each figure, the axes are indicated by arrows.
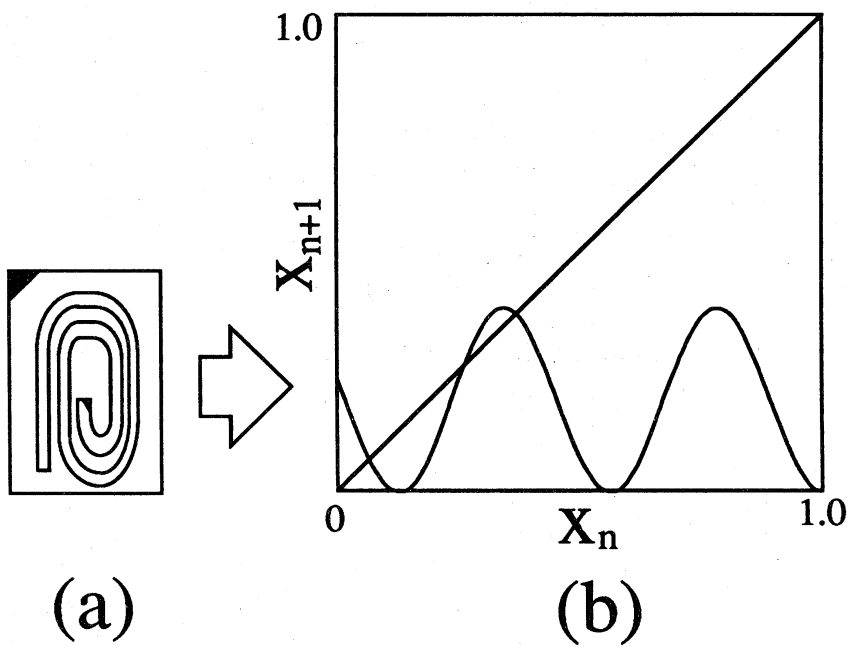
Figure 9 (a) Schematic model of the attractor formation.
(b) One-dimensional map model.
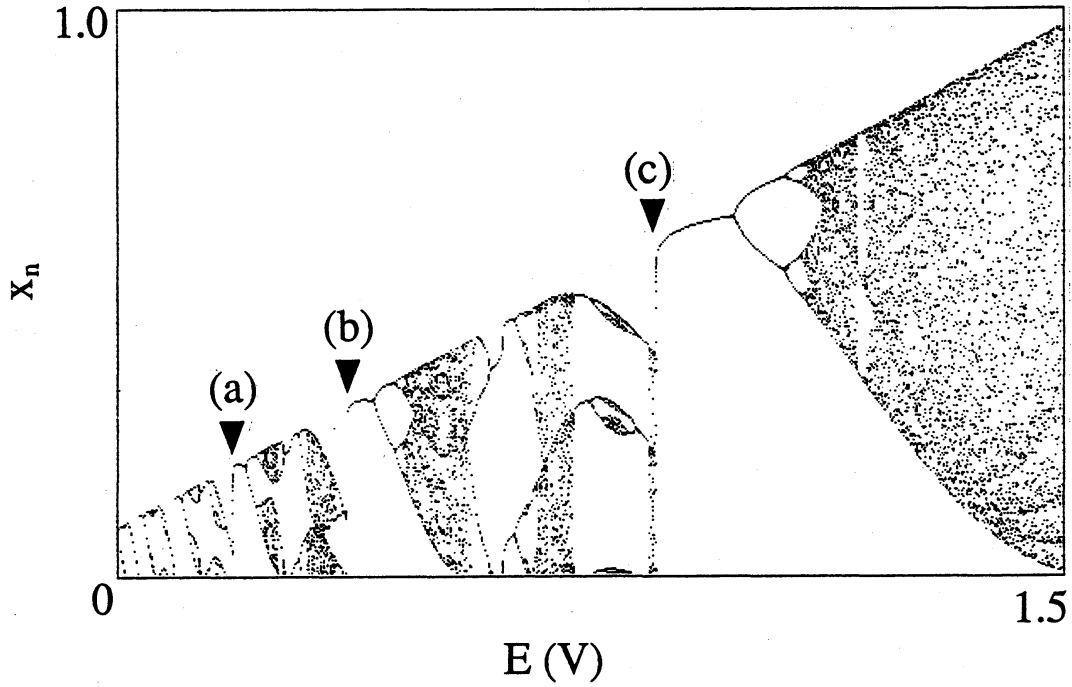
Figure 10 One-parameter bifurcation diagram of the one-dimensional map.
0 V ≤ E ≤ 1.5 V, f = 35 kHz.
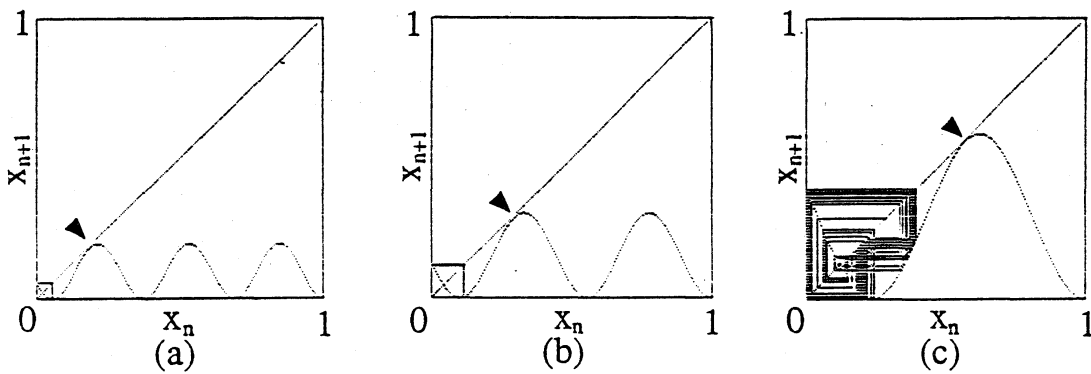
Figure 11 Orbits of the one-dimensional map.
(a) E = 0.18 V. (b) E = 0.36 V. (c) E = 0.85 V.